ORIGINAL RESEARCH

Engineered, Radially Aligned, Gradient-Metformin-Eluting Nanofiber Dressings Accelerate Burn-Wound Healing

Shih-Heng Chen[1],*, Hsiao-Jui Kuo[1],*, Pang-Yun Chou[2], Chia-Hsuan Tsai[3], Shih-Hsien Chen[1], Yi-Chen Yao[4], Shih-Jung Liu ⓘ[4,5]

[1]Department of Plastic and Reconstructive Surgery, Chang-Gung Memorial Hospital, Chang-Gung University and Medical College, Taoyuan, Taiwan; [2]Department of Plastic and Reconstructive Surgery and Craniofacial Research Center, Chang Gung Memorial Hospital at Linkou, Taoyuan, 33305, Taiwan; [3]Department of Plastic and Reconstructive Surgery, Chang-Gung Memorial Hospital, Keelung Branch, Chang-Gung University and Medical College, Keelung, Taiwan; [4]Department of Mechanical Engineering, Chang Gung University, Taoyuan, 33302, Taiwan; [5]Department of Orthopedic Surgery, Bone and Joint Research Center, Chang Gung Memorial Hospital at Linkou, Taoyuan, 33305, Taiwan

*These authors contributed equally to this work

Correspondence: Shih-Jung Liu, Mechanical Engineering, Chang Gung University, 259, Wen-Hwa 1st Road, Kwei-Shan, Tao-Yuan, 33302, Taiwan, Tel +886-3-2118166, Fax +886-3-2118558, Email shihjung@mail.cgu.edu.tw

Introduction: Deep, second- and third-degree burn injuries may lead to irreversible damage to the traumatized tissue and to coagulation or thrombosis of the microvessels, further compromising wound healing. Engineered, morphologically gradient drug-eluting nanofiber dressings promote wound healing by mimicking tissue structure and providing sustained drug delivery, which is particularly beneficial for wound management.
Methods: This study exploited a resorbable, radially aligned nanofiber dressing that provides the sustained gradient release of metformin at the wound site using a pin-ring electrospinning technique and a differential membrane-thickness approach.
Results: The experimental results suggested that the electrospun nanofibrous dressings exhibited uniform and radially oriented fiber distributions. In vitro, these dressings offered an extended release of metformin for 30 d. The incorporation of water-soluble metformin significantly enhanced the hydrophilicity of the nanofiber membranes. Moreover, the in vivo burn-wound-healing model of rats showed that the radially aligned gradient metformin-eluting poly(lactic-co-glycolic acid) (PLGA) nanofibers exhibited significantly superior healing capability compared to the pristine PLGA, metformin-eluting, and control dressings. Histological images showed that the mesh/nanofibers produced no adverse effects.
Conclusion: The findings in this study emphasize the potential of resorbable, radially aligned nanofiber dressings as advanced wound care solutions, offering broad applicability and meaningful clinical impact.
Keywords: wound dressings, radially aligned membranes, gradient metformin release, nanofibers, needle-ring electrospinning

Introduction

Skin, a part of the integumentary system, is the largest organ in the human body and defends us from microorganisms and maintains body temperature and body fluid. However, physical injury, surgery, or an underlying medical condition can cause disruptions in the continuity of skin or underlying tissues and subsequent wound formation. Burns are one of the most common physical injuries to the skin and can be caused by flames, scalds, chemicals, or electricity. A global analytic study found that there were nearly 9 million new burn injury cases in 2019 in the worldwide.[1] In addition to an annual mortality approximating 180,000 according to the world health organization, an average total healthcare cost of approximately 88000 US dollars for burn patients was reported in a systemic review.[2] To manage these burn wounds of varying degrees, topical medicine treatments and special dressings were used with both clinical and socioeconomical outcomes. First-degree, superficial, burn injuries usually heal by themselves but severe, second- or third-degree burns

may lead to irreversible damage to the traumatized tissue and coagulation or thrombosis of the microvessels. During burn injury, many small blood vessels may coagulate or form clots directly due to the heat, leading to subsequent tissue hypoxia, dehydration, and loss of nutrition sources. This further results in compromised, wound healing and increased infection risk.

Burn-wound healing is a dynamic and complex procedure consisting of multiple phases; each phase is composed of a series of cellular and molecular events. Burn-wound healing typically involves four overlapping phases: hemostasis, inflammation, proliferation, and remodeling.[3] The hemostasis phase involves the immediate response to the injury, wherein blood vessels constrict to minimize blood loss, followed by blood clot formation to seal the wound. In the inflammation phase, immune cells infiltrate the wound to remove debris, pathogens, and damaged tissues. In the proliferation phase, new tissues are generated, and the wound closes gradually as granulation tissues are formed and collagen is synthesized. Finally, in the remodeling phase, the newly formed tissues undergo maturation and remodeling to restore strength and functionality to the affected area.[4]

Effective wound management is essential to facilitate the healing process and prevent complications such as infections and delayed healing.[5–10] Dressings play a critical role in wound care by creating a conducive environment for optimal, wound healing.[11] Among the various dressing designs explored previously, a notable concept is that of the radial alignment of the dressing fibers.[12] In this approach, the alignment of the dressing fibers mimics the natural, extracellular matrix (ECM), promoting superior cell adhesion and the proliferation of human-adipose-derived mesenchymal stem cells that are crucial for wound healing. Shin et al[13] reported that radially patterned polycaprolactone nanofibers (fabricated using a modified electrospinning method) exhibit mechanical properties similar to those of conventional fibers and possess enhanced biological functionality. The radial alignment of the dressing fibers expedites cellular migration from the wound edge toward the center, surpassing the pace of random deposition and facilitating faster, tissue regeneration.

Drug-loaded resorbable dressings significantly advance wound care by offering the targeted delivery of therapeutic agents directly to the wound site.[14] Such dressings provide a protective barrier against external contaminants and deliver medications or bioactive compounds that can promote healing and prevent infection. Furthermore, these drug-loaded dressings enable the sustained release of therapeutic agents, ensuring prolonged exposure to the wound bed while minimizing systemic side effects. In addition, the versatility of drug-loaded dressings allows customization based on specific wound needs; thus, they are a valuable tool in modern, wound-management strategies.[15–17] These dressings also possess the required flexibility to facilitate surface applications. Finally, the dressings are resorbable after fulfilling their function and exhibit biocompatibility to ensure that the degradation process of the material does not contribute to tissue irritation.[18–20]

Metformin belongs to a class of drugs named biguanides, which influence the amount of glucose produced by the liver and improve the insulin sensitivity in the cells.[21,22] This medication is typically prescribed to treat type-2 diabetes. When metformin is integrated into dressings, it can target cytokines to augment wound healing by specifically addressing pro-inflammatory cytokines, such as interleukin-1β (Il-1β) and tumor necrosis factor-α (TNF-α), thus limiting their expression. This anti-inflammatory mechanism and its angiogenic potential accelerate wound healing, especially during the initial stages. Understanding how metformin modulates cytokine responses is pivotal for developing effective wound dressings. To this end, Liao et al[23] employed a dressing with a "sandwich-like" structure of electrostatically spun nanofiber, which comprised the hydrophobic material as an outer layer and metformin as an inner layer, for wound dressing. The protracted release time of metformin is instrumental in promoting the healing of diabetic wounds. Building on this premise, the gradient release of a delivered drug is expected to serve as a guided cue for cell migration, thereby enhancing wound healing. Although the literature on this subject is limited, it presents a promising avenue for innovation in wound dressing. Though topical metformin use has been proposed in chronic, diabetic wounds, there were few reports on the efficacy of topical metformin on burn wounds. The major challenge of acute, burn-wound treatment was the deteriorated-tissue microenvironment—ECM loss, severe inflammatory reaction, angiogenesis impairment, and infection. Shi et al found that metformin could reduce dermal thickness, deposition of collagen I, as well as mRNA expression of IL1β and CC chemokine ligand 2 (CCL2) in burn wounds on rats in vivo.[24] However, further evaluation of the wound-healing process and clinical-dressing design based on the drug effect are necessary. A recent article reported that a hydrogel containing metformin hydrochloride was applied on burn wounds with promising results.[25]

In this study, we exploited a resorbable, radially aligned nanofibrous dressing made of poly(lactic-co-glycolic acid) (PLGA),[26,27] which provides both sustained and gradient release of metformin at the burn wound site. This was achieved using a pin-ring electrospinning technique and a differential membrane thickness approach. The tensile properties of the developed nanofibrous membranes were evaluated. The morphologies of the drug-incorporated nanofibers were characterized using a stereomicroscope and scanning electron microscopy (SEM). Furthermore, the in vitro release profiles of metformin, from the nanofibers, were assessed using high-performance liquid chromatography (HPLC). Finally, the in vivo efficacy of nanofibrous dressings in burn-wound repair was assessed using histological assays on a rat model.

Materials and Methods
Materials
The nanofiber material, PLGA with a LA:GA of 50:50 and a molecular weight of 33 kDa, was sourced from Sigma-Aldrich, MO, USA. The solvent, hexafluoroisopropanol (HFIP), and metformin were also acquired from Sigma-Aldrich.

Fabrication of Radially Aligned Gradient-Metformin-Eluting Membrane
A radially aligned, nanofibrous membrane was fabricated using the pin-ring electrospinning device shown in Figure 1A, which comprises a high-voltage generator, syringe pump, and collector. The collector comprises a metallic ring (ring electrode) with a diameter of 3.5 cm and a metallic pin (point electrode). In total, 1,400 mg of PLGA was dissolved in 5 mL of HFIP. The solution was then electrospun into radially aligned nanofibers. The delivery speed of the solution was 0.7 mL/h, and the applied voltage was 17 kV. The distance between the syringe and the collector was 15 cm.

The gradient-metformin-eluting nanofibers were prepared taking a differential membrane thickness approach; the PLGA and metformin were mixed with HFIP in various weight ratios of 4:1, 6:1, 7:1, 8:1, and 10:1. The compositions of the metformin-loaded nanofibers are listed in Table 1.

Subsequently, the solutions were electrospun using the device in Figure 1B, which comprises a high-voltage generator, syringe pump, and plate collector. The delivery speed of the mixture was set to 0.8 mL/h, with an applied voltage of 17 kV, and a distance of 15 cm between the spinning nozzle and the collection plate. Three plastic templates with hole diameters of 1.5, 2.5, and 3.5 cm were positioned approximately 5 mm in front of the plate collector to achieve a gradient distribution of metformin throughout the nanofibrous membranes. Following three consecutive electrospinning processes using templates of varying hole sizes, a circular membrane with three zones (inner, middle, and outer diameters of 1.5, 2.5, and 3.5 mm, respectively) was obtained. Three types of metformin-eluting nanofibrous membranes with different PLGA/metformin ratios (4:1, 6:1, and 8:1 for the inner zone; 4:1, 7:1, and 10:1 for the middle zone; and 4:1 for the outer zone) were obtained via electrospinning. The thickness of the inner zone of the electrospun membranes was approximately 300 μm, whereas that of the outer zone was 100 μm.
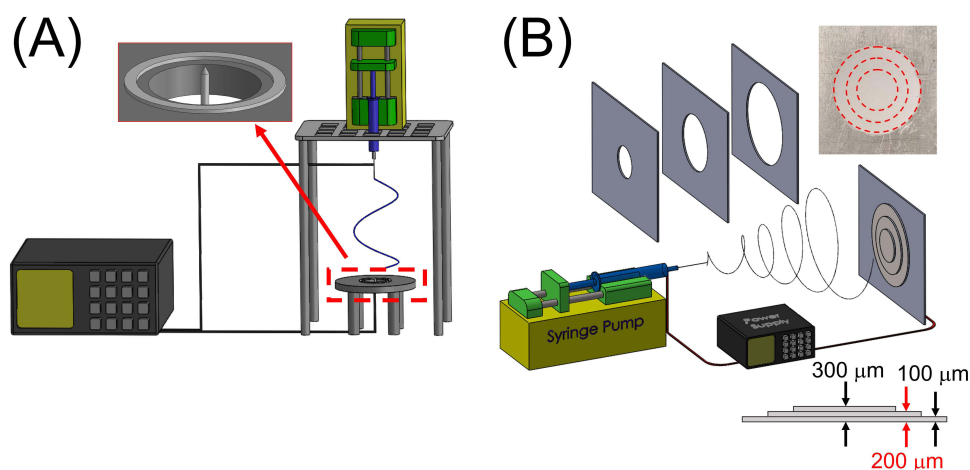

Figure 1 (**A**) Device for electrospinning radially aligned PLGA membranes, (**B**) apparatus for fabricating gradient-metformin-eluting membranes.

Table 1 Composition of Mats with Different PLGA-to-Metformin Ratios

PLGA/drug ratio	PLGA (mg)	Metformin (mg)	HFIP (mL)
4:1	560	140	2.5
6:1	600	100	2.5
7:1	612.5	87.5	2.5
8:1	622.7	77.7	2.5
10:1	636.4	63.6	2.5

After spinning, the radially aligned nanofibrous membrane and the gradient metformin distribution membrane were combined into a single membrane. The membrane samples were subjected to a chamber maintained at 40 °C for three days to allow for the vaporization of the solvent. Subsequently, the samples were stored at 4 °C until use.

Microscopic Observations

The electrospun nanofibrous membranes were evaluated for their morphological structure using a stereomicroscope (WF10X, Pentad Corp., Taipei, Taiwan) and a JEOL Model JSM-7500F FESEM (Tokyo, Japan) after spinning and solvent vaporization. The samples were gold-coated prior to SEM observation. To determine the size allocation, 50 nanofibers were selected arbitrarily and analyzed using ImageJ software (national institutes of health, Bethesda, MD, USA). This analysis was conducted in triplicate (N = 3) to ensure the accuracy and reliability of the results.

Mechanical Properties

The tensile properties of the metformin-eluting nanofibrous membranes were evaluated using a tensile testing machine (Lloyd, Ametek, USA) equipped with a 2.5 kN load cell. The extending rate was maintained at 60 mm/min, and measurements of the maximum strength and deformation were monitored during testing.

Contact Angle of Water

The contact angles of unfilled PLGA and metformin-infused nanofibers were measured to examine hydrophilicity. Waterdrops were gradually introduced to the nanofiber surface (20 mm × 20 mm), and each was evaluated by a monitor. Three analyses were performed (N = 3).

Fourier Transform Infrared Spectroscopy

In total, 32 infrared scans of the metformin-loaded membranes were obtained via Fourier transform infrared (FTIR) spectroscopy using the Bruker Tensor 27 spectrometer with a 4 cm^{-1} resolution in the absorption mode. The nanofibrous specimen was compressed into KBr discs, and the absorption spectrum was monitored in the range of 400–4000 cm^{-1}.

Differential Scanning Calorimetry

Differential scanning calorimetry (DSC) analysis was conducted to investigate the thermal properties of both pure PLGA and the metformin-loaded PLGA nanofibers. The specimens were heated from 30–300 °C at a rate of 10 °C/min using a DSC instrument (TA Instruments, New Castle, DE, USA).

In vitro Release of Metformin

The release profiles of metformin from the nanofibrous membranes were investigated using an in vitro elution scheme. Circular samples, each with a diameter of 4 mm, were extracted from the inner, middle, and outer zones of the membranes. These samples (N = 3) were then placed in assay tubes containing 1 mL of phosphate-buffered saline

11466
DovePress

International Journal of Nanomedicine 2024:19

(PBS) and maintained at 37 °C for 24 h. After incubation, the mixtures were collected and evaluated. Subsequently, new PBS (1 mL) was added to the tubes for the next 24-hour incubation period, and this procedure was repeated for 30 d.

HPLC was utilized to assess the metformin concentration in each mixture. The analysis was conducted using a Hitachi L-2200R multi-solvent delivery system (Tokyo, Japan). An Inertsil C18 column (250 mm × 4.6 mm, 5 μm) was used to separate the metformin. The mobile phase consisted of PBS (pH = 5.73): acetonitrile (35:65, v/v). The absorbance was monitored at a wavelength of 233 nm and a flow rate of 1.0 mL/min. The retention time was set to 2.6 min.[28,29]

In vivo Animal-Related Experiment

Sprague–Dawley rats weighing approximately 300 g were used and following the guidelines of the National Institute of Health of Taiwan, a licensed veterinarian supervised their treatment and care. All animal-related processes in this study received approval from the institutional animal care and use committee of Chang Gung Memorial Hospital (IACUC Approval No.: 2,022,121,922). After administering anesthesia, two, full-thickness, circular, burn wounds (2 cm in diameter), lateral to the vertebral transverse processes, were prepared on the back of each rat, by applying a 150°C copper bar to the skin for 40s to create a full-thickness burn. The eschar was removed 48 h later and the rats were treated according to different group designs. The rats were divided into four groups of five rats each. Those in the control group were treated with a conventional gauze sponge, which served as the control. Electrospun, pristine PLGA nanofibers were applied to the wounds of each rat in the PLGA group, metformin-loaded PLGA nanofibers were applied to each rat wound in the PLGAM group, and radially aligned PLGA nanofibers loaded with metformin were applied to the rats in the PLGAMRA group. The gross photographs of the wounds were captured to evaluate the wound area, 3, 7, 14, 21, and 28 d post-operation. In addition, histological examinations of the wounds were performed at 7 and 28 d post-operation.

Statistics and Data Analysis

Quadruplicate samples were evaluated, and the data were analyzed using one-way analysis of variance (ANOVA). Statistical significance was determined at p values < 0.05.b.

Results

Characterization of Nanofibrous Membranes

Figure 2A and B show the PM and SEM images of a typical scaffold involving electrospun PLGA nanofibers with radial alignment spanning the void gap between the metal pin and the ring. These images suggest that the fibers were radially aligned from the center of the dressing to the periphery.

Figure 3 shows SEM images and fiber size distributions of the electrospun nanofibers of virgin PLGA and metformin-loaded nanofibers with various PLGA-to-metformin ratios.

The inclusion of metformin reduced the size distribution of the nanofibers. During the electrospinning process, the polymer/drug solution was stretched by the external force generated by the electric field. The polymer acts as the primary component in resisting this stretching force. The incorporation of metformin reduced the polymer content in the solution, making it easier for the solution to be extended. As a result, the diameter of the electrospun nanofibers decreased accordingly.

Figure 4 illustrates the stress–strain profiles of the virgin PLGA and metformin-incorporated PLGA nanofibers.

The addition of metformin increases the ultimate strength while decreasing the elongation at break. The inclusion of metformin lowers the polymer content in the solution, allowing it to stretch more easily. This higher stretching rate tends to orient the polymer molecular chains along the axial direction, enhancing the tensile strength. However, the added metformin acts as a filler with inferior extensibility in the polymer/drug composites, which in turn leads to reduced strain before failure in the nanofibrous mat. However, all the nanofibers displayed good extension (> 50%) before fracture.

Figure 5 shows the water contact angles of the virgin PLGA and metformin-loaded PLGA nanofibrous membranes. The measured contact angles were 129.99±7.76°, 56.07±4.32°, 77.04±2.06°, 84.53±5.18°, 95.92±6.86°, and 113.22±8.98°,
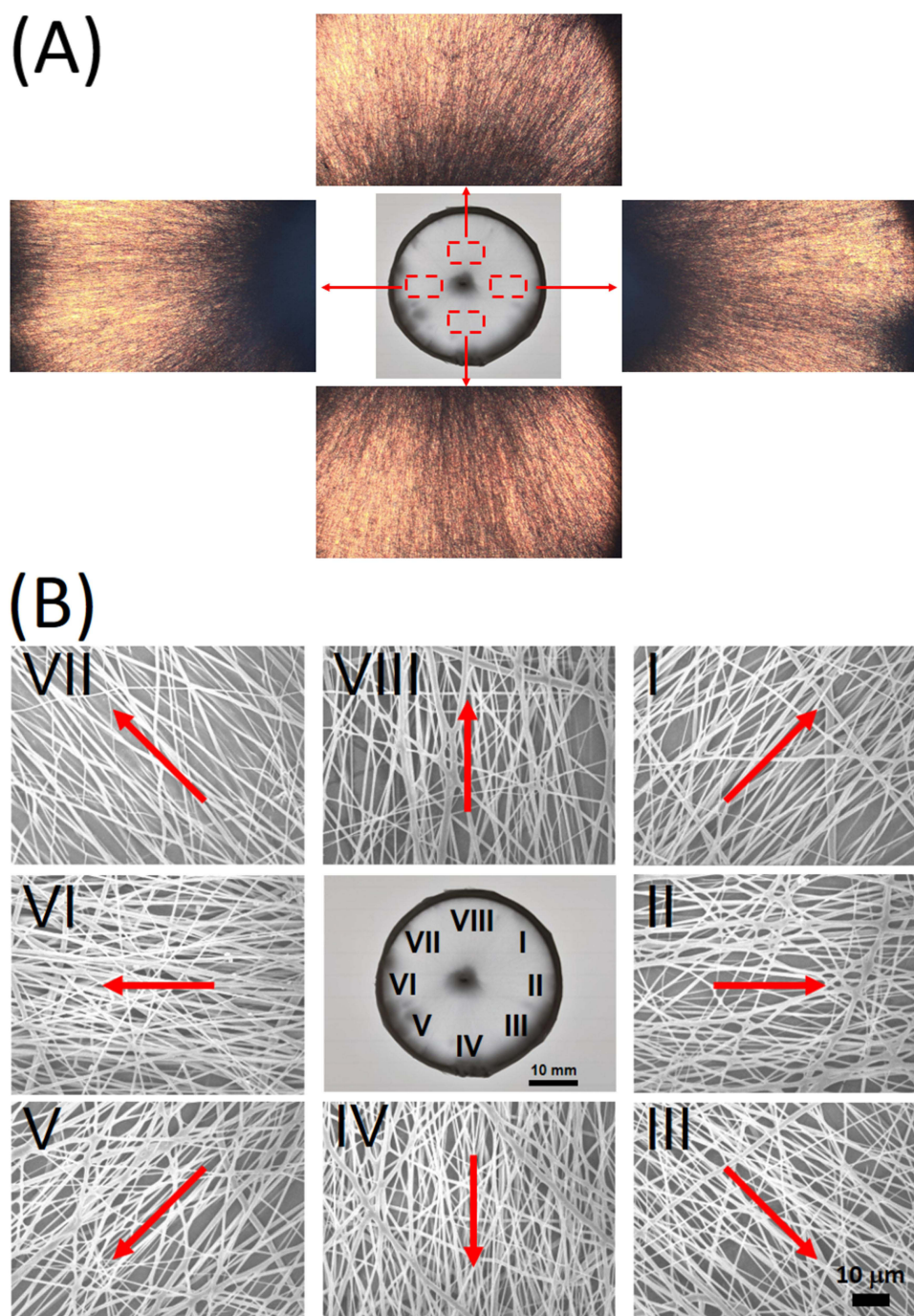
Figure 2 (**A**) Projector microscopy and (**B**) scanning electron microscopy (SEM) images of radially aligned nanofibrous membranes. (The arrows indicate the orientation of the fibers in the radial direction.).

respectively, for pure PLGA and PLGA/metformin ratios of 4:1, 6:1, 7:1, 8:1, and (F) 10:1 nanofibrous mats. Clearly, the inclusion of water-soluble metformin enhances the hydrophilicity of the PLGA nanofibers.

The data in Figure 6A illustrate that the new peaks at 3370, 3183, and 1582 cm^{-1} resulted from the –NH bond of the added pharmaceuticals.[30,31] In addition, the C=N peaks at 1638 cm^{-1} developed significantly in relation to the pure PLGA nanofibrous membranes. The thermal behaviors of the pristine PLGA and metformin-loaded PLGA are also assessed, and the results are shown in Figure 6B. The endothermic peak of metformin at 237°C diminished after incorporation into the PLGA matrix, whereas the glass transition temperature of PLGA at 48°C was not observed in the
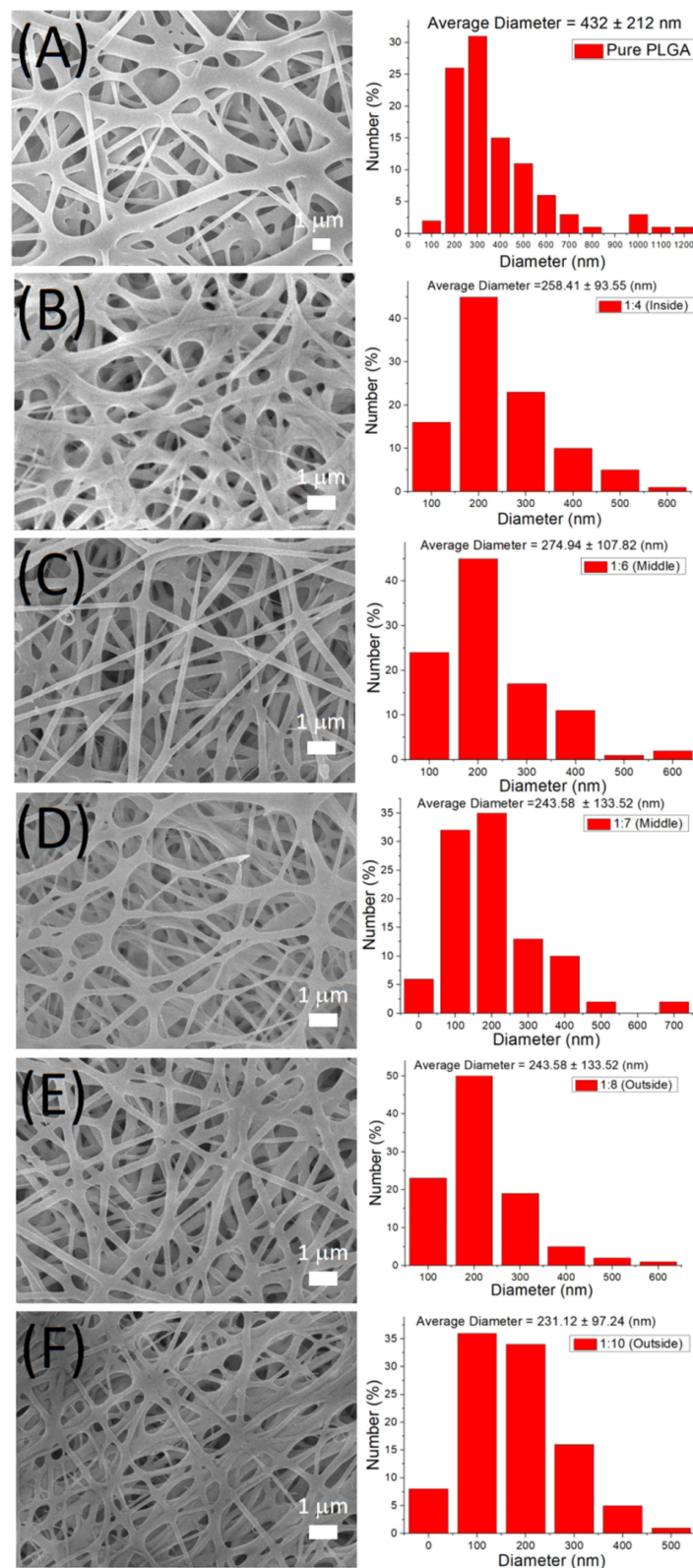
Figure 3 SEM images and fiber diameter distribution of (**A**) virgin PLGA and PLGA/metformin ratios of (**B**) 4:1, (**C**) 6:1, (**D**) 7:1, (**E**) 8:1, and (**F**) 10:1 nanofibrous membranes.
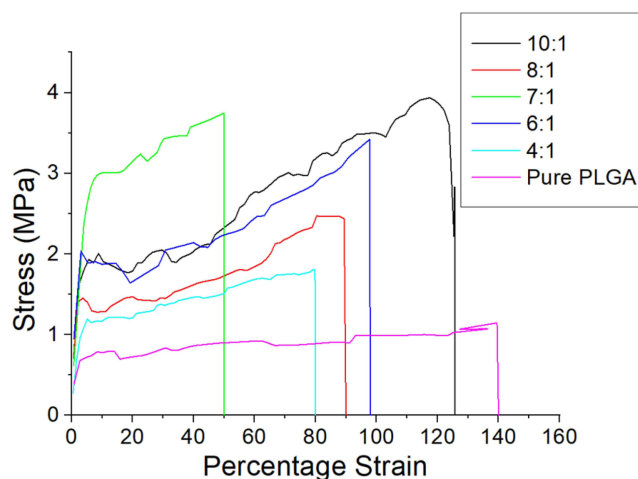
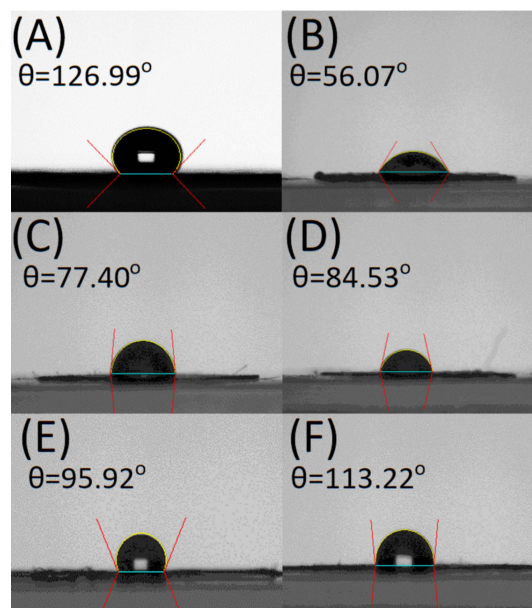**Figure 4** Tensile properties of electrospun PLGA/metformin nanofibers.

Figure 5 Water contact angles of (**A**) pure PLGA, and PLGA/metformin ratios of (**B**) 4:1, (**C**) 6:1, (**D**) 7:1, (**E**) 8:1, and (**F**) 10:1 nanofibrous mats.

PLGA/metformin nanofibers.[32,33] These results indicate the successful embedding of metformin into the PLGA nanofibers.

In vitro Drug Release

Figure 7 revealed the daily and cumulative liberation profiles of the three types of combination membranes. All the different combinations of membranes exhibited gradient drug release behaviors, with the maximum drug concentration at the inner zone and the minimum drug release at the outer zone.

The 4:1, 6:1, and 8:1 combination membranes exhibited a triphasic release feature; that is, a burst on day 1, a secondary high release approximately around day 7, accompanied by a gradual decrease over 30 d. The 4:1, 7:1, and 10:1 combination membranes displayed biphasic discharge, that is, a burst at 1 d and a steady and progressively decreasing release for 30 d. The 4:1 combination membranes showed a triphasic elution pattern, with a burst at 1 d, a second peak release from 7 to 15 d, and a steady low drug release profile until 30 d. Overall, the nanofibrous membranes provided the sustained release of metformin for more than 30 d.
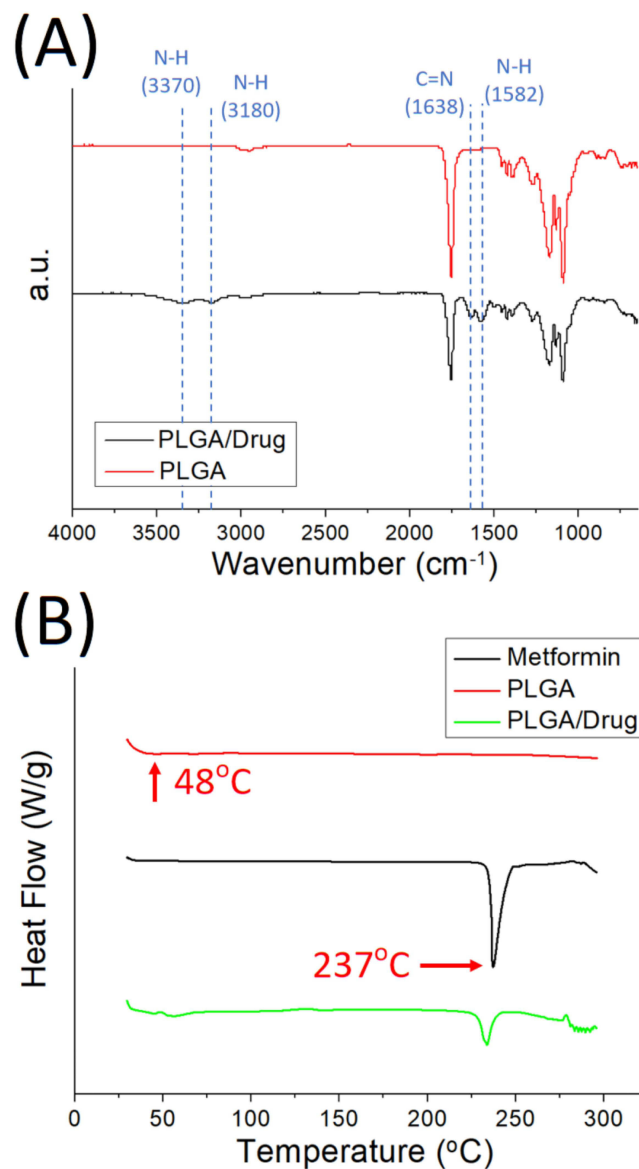
Figure 6 (**A**) Fourier-transform infrared spectroscopy (FTIR) spectra, and (**B**) differential scanning calorimetry (DSC) of PLGA, metformin, and metformin-loaded PLGA nanofibers.

In vivo Results and Histology Assay

Figure 8 illustrates the in vivo efficacy of the various dressings in the rats. On the third day, no significant difference was observed among the various groups. The PLGAMRA group evidenced significantly superior healing to the PLGA, PLGAM, and control groups ($p < 0.05$) 7 d post-implantation. On day 14, the PLGAMRA group exhibited superior healing compared with the PLGA and control groups ($p < 0.05$). On days 21 and 28, the PLGAMRA group showed significantly improved healing than the control group ($p < 0.05$). These findings demonstrate the excellent wound repair capability of PLGAMRA dressings.

Figure 9 displays the hematoxylin and eosin (HE) as well as Masson's trichrome (MT) micro-images of the nanofibrous dressings. Additionally, the histological micro-images captured on days 7 and 28 post-operation showed no signs of increased inflammation, leukocytes, or tissue necrosis in any of the groups. Additionally, no adverse effects were observed in the histological images.
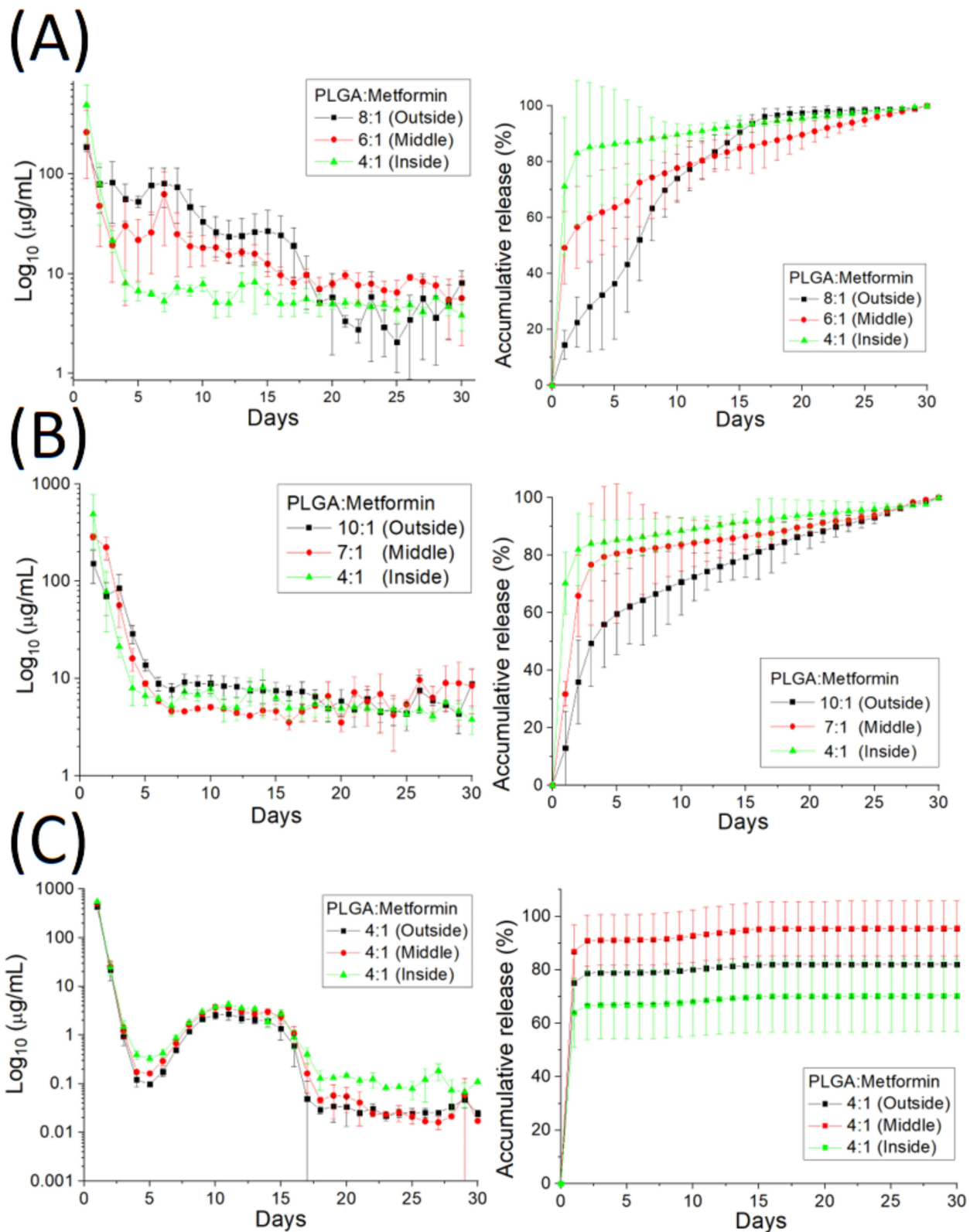
Figure 7 In vitro daily (left) and cumulative (right) release of metformin from nanofibers, with PLGA ratios of (**A**) 8:1, 6:1, and 4:1 for the outer, middle, and inner layers, respectively; (**B**) 10:1, 7:1, and 4:1 for the outer, middle, and inner layers, respectively; and (**C**) 4:1 for all layers.
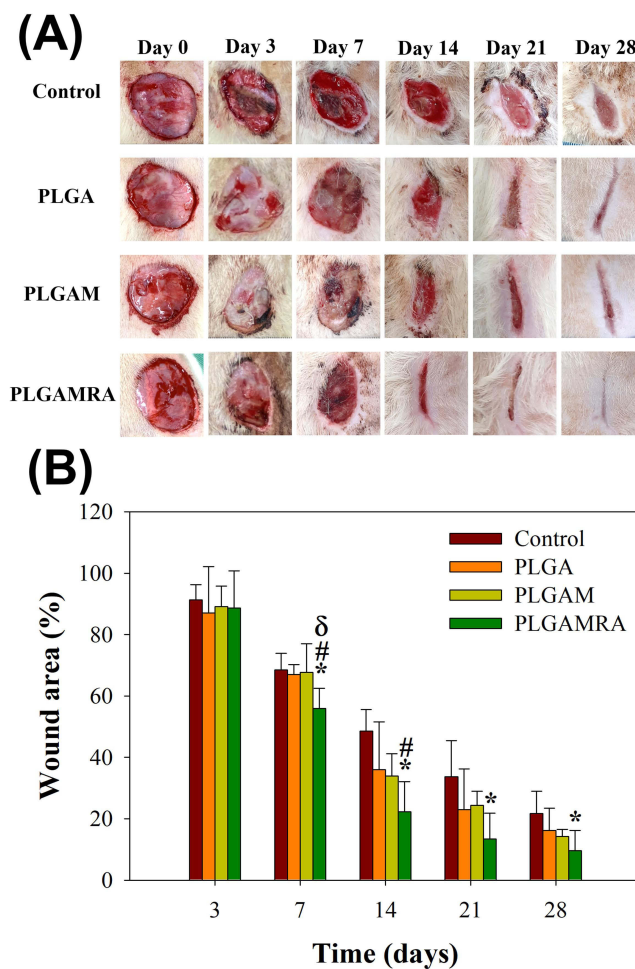
Figure 8 Effects on wound healing in rats for different groups at identical time points: (**A**) Representative photographs of wound healing, and (**B**) quantitative results of wound healing area. *indicates $p < 0.05$ compared with the control group; # indicates $p < 0.05$ compared with the PLGA group; δ indicates $p < 0.05$ compared with the PLGAM group.

Discussion

This study developed resorbable, radially aligned nanofibrous dressings that provide a sustained gradient release of metformin to the target wound site. Compared to previously developed dressings in the literature,[16,18,19,22,26,27] these radially aligned, gradient-metformin-eluting nanofibers offer several advantages for promoting cell proliferation and wound healing. They provide a structural framework that mimics the native ECM, promoting cell adhesion and alignment along the fibers, benefiting the cells related to wound healing, such as fibroblasts and keratinocytes. The porous nanofiber structure also enables efficient diffusion of nutrients and oxygen to the cells within the wound site. This improved oxygenation and nutrient supply creates a favorable microenvironment for cell proliferation and tissue regeneration. Furthermore, the radially aligned nanofibers modulate the cell signaling pathways involved in the wound healing process. Topographical cues provided by nanofiber alignment can activate signaling cascades that promote cell proliferation, migration, and differentiation, leading to accelerated wound closure and tissue regeneration. Finally, the alignment of the nanofibers provided mechanical support and stability to the wound site, preventing tissue collapse and promoting sound tissue formation. This structural reinforcement can reduce the risk of scar formation and improve the overall cosmetic outcomes of wound healing.

Radially aligned nanofibers can also be engineered to incorporate bioactive molecules such as growth factors, cytokines, and antimicrobial agents. The controlled release of these molecules from the nanofiber matrix can enhance cell proliferation, angiogenesis, and tissue remodeling to promote more rapid and effective wound healing. Additionally,
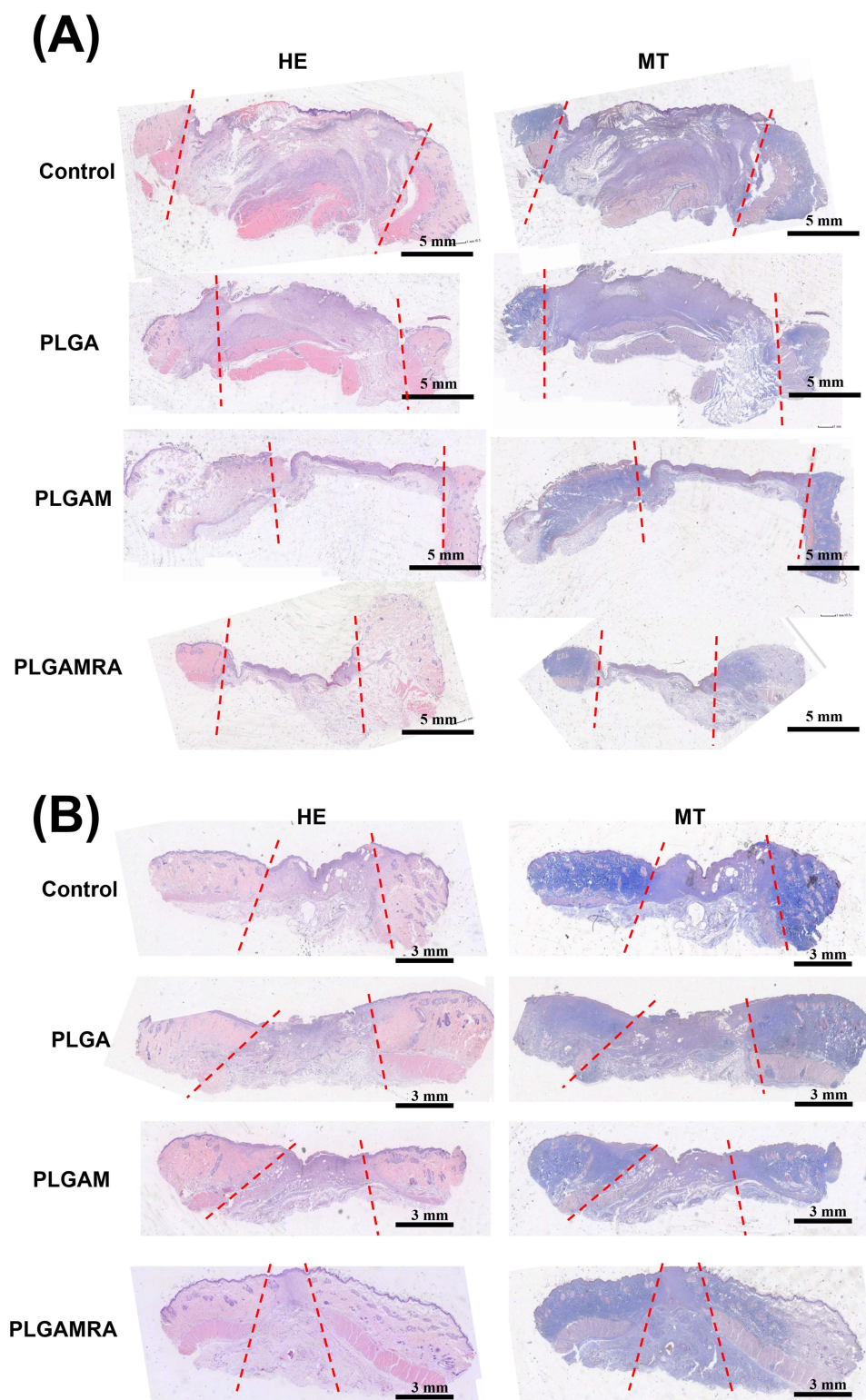
Figure 9 Histological images at (**A**) 7 and (**B**) 28 d post-implantation. No signs of increased inflammation, leukocyte infiltration, or tissue necrosis were observed in any of the groups. Additionally, no adverse effects were noted in the histological images. (The dashed lines depict the central margin of re-epithelialization. The area between the dashed lines shows granulation tissue formation, but full re-epithelialization has not yet occurred.).

when combined with metformin,[24,34] a promising candidate for adjunct therapy, the radially aligned nanofibrous dressings further promote healing for wound management.

The experimental results demonstrated that the PLGA group exhibited better healing capability than the control group at days 3, 7, 14, 21, and 28 post-implantation, even though the difference was not statistically significant ($p > 0.05$). This may be due to the fact that PLGA nanofibers mimic the structure of the ECM, thus accelerating wound healing. Additionally, the PLGAMRA group demonstrated significantly better healing than the PLGA, PLGAM, and control groups ($p < 0.05$) at 7 days post-implantation. By day 14, healing in the PLGAMRA group remained superior to that of the PLGA and control groups ($p < 0.05$). On days 21 and 28, the PLGAMRA group continued to show significantly greater healing compared to the control group ($p < 0.05$). The effects of topical-form metformin on burn-injury wounds and subsequent healing process have been rarely mentioned in the literature. According to one study, there was a suppressive effect of metformin on pro-inflammatory markers by inhibition of several pathways in vitro.[24] Based on their results, they applied a hydrogel containing metformin hydro-chloride on rat burn wounds and revealed superior re-epithelialization compared to the untreated and placebo gel groups.[25] Furthermore, the study also showed a decreased size of burn wounds as the dose of topical metformin application increased. This supports the potential feasibility and rationale of the design of metformin concentration gradient used in our study to accelerate the wound healing.

The local and gradient-drug-release systems enable the controlled release of drugs over time. This sustained release of metformin maintains the therapeutic concentrations at the wound site, promoting optimal, healing conditions without frequent dosing. In addition, by minimizing systemic exposure to medicants, such release systems can reduce the risk of toxicity associated with high, systemic-drug concentrations. This is particularly important for drugs with narrow therapeutic windows and potential adverse effects. Tailoring drug release to match the dynamic stages of wound healing can help optimize the therapeutic effects. Additionally, local drug-delivery systems can offer convenience and improve patient compliance compared with traditional, systemic-drug administration methods. Patients may prefer treatment regimens involving less frequent dosing or invasive procedures. Furthermore, drug-release systems can be customized to suit the specific requirements of different wound types, sizes, and locations. This flexibility allows healthcare providers to tailor treatment strategies to individual patient needs and optimize therapeutic outcomes.

Mukherjee et al suggested that nanofibrous meshes offer a unique topography for entrapping therapeutic cells for up to six weeks, facilitating the significant infiltration of host anti-inflammatory macrophages.[35] Ensuring proper cell attachment to a scaffold is crucial for success. However, the use of highly hydrophobic scaffold dressings can result in suboptimal cell colonization.[36] The experimental findings indicated that incorporating metformin into nanofibrous dressings improved their hydrophilicity and enhanced cell proliferation during wound repair.

There are three distinct stages of medication release from a drug-embedded resorbable dressing or device: burst discharge, diffusion-controlled elution, and degradation-dominated release. Most infused pharmaceuticals are likely to encapsulated in the polymeric matrix during electrospinning. However, a few pharmaceuticals may be placed on the surfaces of certain nanofibrous membranes, causing a burst discharge. Following the initial burst, drug release would be regulated by diffusion and polymer degradation, resulting in a secondary peak in metformin discharge. Subsequently, the release profile would maintain a steady pattern until all encapsulated drugs were fully released. The in vitro results confirmed that the electrospun drug-incorporated dressings released a high concentration of metformin for 30 d, enhancing cell proliferation and wound healing.

Despite the interesting findings of this preliminary study, there were some limitations. While various concentrations of metformin were used in material synthesis, the optimal concentration has not yet been determined. Furthermore, the biosafety of the material remains unverified. Additional research is needed to confirm its ability to promote fibroblast proliferation, support orientational arrangements, and inhibit inflammatory factors. Additionally, this study used a rat model to evaluate the drug-eluting nanofibrous dressings, so the relevance of our findings to human wounds remains unclear and will be addressed in future research. Finally, the transition of the developed nanofibrous dressings from the lab to clinical use—requiring the overcoming of technical, regulatory, and practical hurdles, especially in ensuring scalability, safety, efficacy, and cost-effectiveness—will also be further explored.

Conclusions

We successfully developed resorbable, radially aligned nanofibrous dressings for burn wound healing, utilizing a pin-ring electrospinning technique and a differential membrane thickness approach. Experimental results confirmed that these nanofibrous dressings provide sustained, gradient release of metformin for over 30 days at burn wound sites. The radially aligned, metformin-eluting PLGA nanofibers demonstrated significantly superior healing capabilities compared to pristine PLGA, metformin-eluting, and control dressings. Histological images showed no adverse effects. Overall, these findings underscore the potential of resorbable, radially aligned nanofiber dressings as advanced wound care solutions with broad applicability and significant clinical impact.

Abbreviations

ECM, natural extracellular matrix; PLGA, poly(lactic-co-glycolic acid); SEM, scanning electron microscopy; HFIP, 1,1,1,3,3,3-hexafluoro-2-propanol; FTIR, Fourier transform infrared; DSC, Differential scanning calorimetry; PBS, phosphate-buffered saline; HPLC, high-performance liquid chromatography; ANOVA, analysis of variance; CCL2, CC chemokine ligand 2; PLGAM group, metformin-loaded PLGA nanofibers were applied to each rat wound; PLGAMRA group, radially aligned PLGA nanofibers loaded with metformin were applied to the rats.

Acknowledgments

Disclosure

The authors declare no conflict of interest regarding the publication of this paper.

References

1. Yakupu A, Zhang J, Dong W, Song F, Dong J, Lu S. The epidemiological characteristic and trends of burns globally. *BMC Public Health*. 2022;22(1):1596. doi:10.1186/s12889-022-13887-2
2. World Health Organization, Burns. WHO 2023. Available from: https://www.who.int/news-room/fact-sheets/detail/burns. Accessed November 4, 2024.
3. Guo S, Dipietro LA. Factors affecting wound healing. *J Dent Res*. 2010;89(3):219–229. doi:10.1177/0022034509359125
4. Almadani YH, Vorstenbosch J, Davison PG, Murphy AM. Wound healing: a comprehensive review. *Semin Plast Surg*. 2021;35(3):141–144. doi:10.1055/s-0041-1731791
5. Ghomi ER, Khalili S, Khorasani SN, Neisiany RE, Ramakrishna S. Wound dressings: current advances and future directions. *J Appl Polym Sci*. 2019;136(27):47738. doi:10.1002/app.47738
6. Qi X, Ge Z, Chen X, et al. An immunoregulation hydrogel with controlled hyperthermia-augmented oxygenation and ROS scavenging for treating diabetic foot ulcers. *Adv Funct Mater*. 2024;34(33):2400489. doi:10.1002/adfm.202400489
7. Qi X, Shi Y, Zhang C, et al. A hybrid hydrogel with intrinsic immunomodulatory functionality for treating multidrug-resistant pseudomonas aeruginosa infected diabetic foot ulcers. *ACS Materitla Lett*. 2024;6(7):2533–2547. doi:10.1021/acsmaterialslett.4c00392
8. Qi X, Cai E, Xiang Y, et al. An immunomodulatory hydrogel by hyperthermia-assisted self-cascade glucose depletion and ROS scavenging for diabetic foot ulcer wound therapeutics. *Adv Mater*. 2023;35(48):2306632. doi:10.1002/adma.202306632
9. Miller MI, Brightman AO, Epstein FH, et al. BME 2.0: engineering the future of medicine. *BME Frontiers*. 2023;4:001. doi:10.34133/bmef.0001
10. Zhang W, Liu W, Long L, et al. Responsive multifunctional hydrogels emulating the chronic wounds healing cascade for skin repair. *J Control Release*. 2023(354):821–834.
11. Hamed SH, Azooz EA, Al-Mulla EAJ. Nanoparticles-assisted wound healing: a review. *Nano Biomed Eng*. 2023;15(4):425–435. doi:10.26599/NBE.2023.9290039
12. Wang Q, Ma J, Chen S, Wu S. Designing an innovative electrospinning strategy to generate PHBV nanofiber scaffolds with a radially oriented fibrous pattern. *Nanomaterials*. 2023;13(7):1150. doi:10.3390/nano13071150
13. Shin D, Kim MS, Yang CE, Lee WJ, Roh TS, Baek W. Radially patterned polycaprolactone nanofibers as an active wound dressing agent. *Arch Plast Surg*. 2019;46(5):399–404. doi:10.5999/aps.2019.00626
14. Saghazadeh S, Rinoldi C, Schot M, et al. Drug delivery systems and materials for wound healing applications. *Adv Drug Deliv Rev*. 2018;127:138–166. doi:10.1016/j.addr.2018.04.008
15. Aggarwal D, Kumar V, Sharma S. Drug-loaded biomaterials for orthopedic applications: a review. *J Control Release*. 2022;344:113–133. doi:10.1016/j.jconrel.2022.02.029
16. Liu X, Xu H, Zhang M, Yu DG. Electrospun medicated nanofibers for wound healing: review. *Membranes (Basel)*. 2021;11(10):770. doi:10.3390/membranes11100770
17. Leng T, Wang Y, Cheng W, Wang W, Qu X, Lei B. Bioactive anti-inflammatory antibacterial metformin-contained hydrogel dressing accelerating wound healing. *Biomater Adv*. 2022;135:212737. doi:10.1016/j.bioadv.2022.212737

18. Zhao J, Qiu P, Wang Y, et al. Chitosan-based hydrogel wound dressing: from mechanism to applications, a review. *Int J Biol Macromol*. 2023;244:125250. doi:10.1016/j.ijbiomac.2023.125250

19. Rani Raju N, Silina E, Stupin V, Manturova N, Chidambaram SB, Achar RR. Multifunctional and smart wound dressings-A review on recent research advancements in skin regenerative medicine. *Pharmaceutics*. 2022;14(8):1574. doi:10.3390/pharmaceutics14081574

20. Marroquin-Garcia R, Royakkers J, Gagliardi M, et al. Polyphosphate-based hydrogels as drug-Loaded wound dressing: an in vitro sStudy. *ACS Appl Polym Mater*. 2022;4(4):2871–2879. doi:10.1021/acsapm.1c01533

21. Foretz M, Guigas B, Viollet B. Metformin: update on mechanisms of action and repurposing potential. *Nat Rev Endocrinol*. 2023;19(8):460–476. doi:10.1038/s41574-023-00833-4

22. Shurrab NT, Arafa EA. Metformin: a review of its therapeutic efficacy and adverse effects. *Obes Med*. 2020;17:100186. doi:10.1016/j.obmed.2020.100186

23. Liao M, Jian X, Zhao Y, et al. "Sandwich-like" structure electrostatic spun micro/nanofiber polylactic acid-polyvinyl alcohol-polylactic acid film dressing with metformin hydrochloride and puerarin for enhanced diabetic wound healing. *Int J Biol Macromol*. 2023;253(Pt 6):127223. doi:10.1016/j.ijbiomac.2023.127223

24. Shi L, Jiang Z, Li J, et al. Metformin improves burn wound healing by modulating microenvironmental fibroblasts and macrophages. *Cells*. 2022;11 (24):4094. doi:10.3390/cells11244094

25. Ozyilmaz ED, Celikkaya R, Comoglu T, Ozakpinar HR, Behzatoglu K. In vitro and in vivo evaluation of metformin hydrochloride hydrogels developed with experimental design in the treatment of burns. *AAPS Pharm Sci Tech*. 2023;24(8):248. doi:10.1208/s12249-023-02704-7

26. Hua Y, Su Y, Zhang H, et al. Poly(lactic-co-glycolic acid) microsphere production based on quality by design: a review. *Drug Deliv*. 2021;28 (1):1342–1355. doi:10.1080/10717544.2021.1943056

27. Pardeshi SR, Nikam A, Chandak P, Mandale V, Naik JB, Giram PS. Recent advances in PLGA based nanocarriers for drug delivery system: a state of the art review. *Int J Polym Mater*. 2023;72(1):49–78. doi:10.1080/00914037.2021.1985495

28. Gedawy A, Al-Salami H, Dass CR. Development and validation of a new analytical HPLC method for simultaneous determination of the antidiabetic drugs, metformin and gliclazide. *J Food Drug Anal*. 2019;27(1):315–322. doi:10.1016/j.jfda.2018.06.007

29. Chhetri HP, Thapa P, Van Schepdael A. Simple HPLC-UV method for the quantification of metformin in human plasma with one step protein precipitation. *Saudi Pharm J*. 2014;22(5):483–487. doi:10.1016/j.jsps.2013.12.011

30. Jagdale S, Patil S, Kuchekar B, Chabukswar A. Preparation and characterization of metformin hydrochloride - Compritol 888 ATO Solid Dispersion. *J Young Pharm*. 2011;3(3):197–204. doi:10.4103/0975-1483.83758

31. Sabbagh BA, Kumar PV, Chew YL, Chin JH, Akowuah GA. Determination of metformin in fixed-dose combination tablets by ATR-FTIR spectroscopy. *Chem Data Collect*. 2022;39:100868. doi:10.1016/j.cdc.2022.100868

32. Kim DW, Park JB. Development and pharmaceutical approach for sustained-released metformin succinate tablets. *J Drug Deliv Sci Tec*. 2015;30:90–99. doi:10.1016/j.jddst.2015.09.019

33. Bouriche S, Alonso-Garcia A, Carceles-Rodriguez CM, Rezgui F, Fernandez-Varon E. An in vivo pharmacokinetic study of metformin micro-particles as an oral sustained release formulation in rabbits. *BMC Vet Res*. 2021;17(1):315. doi:10.1186/s12917-021-03016-3

34. Han X, Tao Y, Deng Y, Yu J, Sun Y, Jiang G. Metformin accelerates wound healing in type 2 diabetic db/db mice. *Mol Med Rep*. 2017;16 (6):8691–8698. doi:10.3892/mmr.2017.7707

35. Mukherjee S, Darzi S, Rosamilia A, et al. Blended nanostructured degradable mesh with endometrial mesenchymal stem cells promotes tissue integration and anti-inflammatory response in vivo for pelvic floor application. *Biomacromolecules*. 2019;20(1):454–468. doi:10.1021/acs.biomac.8b01661

36. Wang W, Caetano G, Ambler WS, et al. Enhancing the hydrophilicity and cell attachment of 3D printed PCL/graphene scaffolds for bone tissue engineering. *Materials (Basel)*. 2016;9(12):992. doi:10.3390/ma9120992